ELSEVIER

Astroparticle Physics 9 (1998) 203–211

Astroparticle Physics

A search for TeV emission from AE Aquarii

M.J. Lang [a,*], J.H. Buckley [b], D.A. Carter-Lewis [c], M. Catanese [c], M.F. Cawley [d], E. Colombo [e], V. Connaughton [f], D.J. Fegan [g], J.P. Finley [h], J.A. Gaidos [h], G.H. Gillanders [a], A.M. Hillas [i], M.P. Kertzman [j], F. Krennrich [c], R.W. Lessard [h], P. Moriarty [k], J. Quinn [ℓ], H.J. Rose [i], G. Sembroski [h], T.C. Weekes [ℓ]

[a] *Department of Physics, National University of Ireland, Galway, Ireland*
[b] *Department of Physics, Washington University, St. Louis, MO 63130, USA*
[c] *Department of Physics and Astronomy, Iowa State University, Ames, IA 50011, USA*
[d] *Department of Physics, National University of Ireland, Maynooth, Ireland*
[e] *CONAE, Paseo Colón 751, 2do.P. (1063), Argentina*
[f] *NASA, Marshall Space Flight Center, Huntsville, AL 35812, USA*
[g] *Department of Physics, National University of Ireland, Dublin, Ireland*
[h] *Department of Physics, Purdue University, West Lafayette, IN 47907, USA*
[i] *Department of Physics, University of Leeds, Leeds, LS2 9JT, UK*
[j] *Department of Physics, DePauw University, Greencastle, IN 46135, USA*
[k] *School of Science, Galway-Mayo Institute of Technology, Galway, Ireland*
[ℓ] *F.L. Whipple Observatory, Harvard-Smithsonian CfA, P.O. Box, Amado, AZ 85645, USA*

Received 8 January 1998; revised 18 April 1998

Abstract

We have observed the cataclysmic variable AE Aqr for a total of 68.7 hours over the epoch 1991–95 using the Whipple Observatory 10 m gamma-ray telescope. An analysis of these data has revealed no evidence for any steady, pulsed or episodic TeV emission. We have calculated an upper limit for steady emission of 4.0×10^{-12} photons $cm^{-2}s^{-1}$ at an energy threshold of 900 GeV. This is three orders of magnitude less than the flux reported by others during burst activity. Our upper limits for coherent pulsed emission at the first and second harmonics of the white dwarf frequency are 1.5×10^{-12} photons $cm^{-2}s^{-1}$ in each case. © 1998 Elsevier Science B.V.

PACS: 95.
Keywords: VHE gamma-ray astronomy; Cataclysmic variables; AE Aquarii

1. Introduction

AE AQR is a DQ Her type cataclysmic variable at a distance of $\sim$ 100 pc [1,2]. It consists of a K5 late-type red dwarf and a white dwarf with an orbital period of 9.88 hours. The optical behaviour of AE Aqr exhibits large flares, highly coherent pulsations at F_0 = 30.23 mHz, and quasi-periodic oscillations (QPQ's). The optical magnitude varies from $\sim$ 12.5 in the quiescent state up to $\sim$ 10.0 during flares which can last from minutes to hours. The optical profile at F_0 consists of a double sinusoid with some bridging emission, with most of the power found at the sec-

* Corresponding author; e-mail: mark.lang@ucg.ie.

PII S0927-6505(98)00020-6

ond harmonic $F_1 = 2F_0$. The period is highly stable, the derivative of the pulse period has been measured as 5.6×10^{-14}s s^{-1} [3]. The keV X-ray emission is also pulsed at F_0 and consists of a single broad sinusoid [4]. The modulation at F_0 is generally accepted to be caused by the rotation of the white dwarf. It has the highest known rotation frequency of the DQ Her type cataclysmic variables. The optical QPO's are present only during flaring. Their amplitudes tend to be substantially larger than the coherent modulations and their frequencies are slightly red-shifted from F_0.

The orbital period is sufficiently short that the K5 star fills its Roche lobe and transfers mass to its partner. The accreting gas may form an accretion disk around the white dwarf. The coherent pulsations are possibly caused by the magnetised white dwarf accreting mass onto its two magnetic poles, whereas the QPO's may arise from an interaction between the white dwarf and inhomogeneities in the accretion disk.

TeV emission has been reported by the Potchefstroom group [5,6]. Their database consists of $\sim$ 277 hours of observations from the epoch 1988–91 and a further 31 hours recorded in 1992–93. They searched for emission at F_0 and at $f_1 = 29.90$ mHz and $f_2 = 30.04$ mHz. The frequencies f_1 and f_2 are representative of the red-shifted QPO range and are separated by one independent Fourier frequency. The most significant signal was found at f_2 and occurred in approximately one in ten observations throughout the database. In simultaneous TeV and optical observations carried out on 20 August 1992, pulsed TeV emission at f_2 appears to be associated with the quiescent optical state. They also report two unpulsed TeV bursts of $\sim$ 1 and $\sim$ 3 min duration on 25 June 1993.

The Durham group have been reported on $\sim$ 100 hours of observations from 1990–91 [7]. They see evidence for pulsed emission at F_1, the second harmonic of the white dwarf frequency, in two out of four monthly data sets, namely October 1990 and August 1991. No activity was seen in data recorded in September and October 1991. A 1 min burst, again pulsed at F_1, was detected on 13 October 1990. In a further 72 hours of data recorded in 1992–93 there is no evidence for persistent low level pulsed emission [8]. However, they did detect a 70 min burst on 11 October 1993 in two independent telescopes. The burst is pulsed at F_1 and is enhanced when simple imaging techniques are used to reject hadron induced events. In the case of both the 1 min and 70 min bursts there is evidence that the signal contains a larger proportion of higher energy events than is observed in the background.

2. Observations and analysis techniques

Our search for TeV emission has been carried out using the atmospheric Cherenkov imaging technique as described by Cawley and Weekes [9]. Data were recorded over the epoch 1991–95 using the Whipple Observatory 10-meter gamma-ray telescope in Southern Arizona. The observations are summarized in Table 1. Typically observations were made at an elevation of 50–55°. The different hardware modes and event selection techniques are discussed below. The instrument has been successfully used to observe TeV emission from the Crab Nebula [10], Markarian 421 [11], and Markarian 501 [12], at high levels of statistical significance. For four nights in October 1992 we have contemporaneous optical observations made by using the nearby 1.2 m optical telescope at the Whipple Observatory.

2.1. Hardware

The instrument, discussed in detail by Cawley et al. [13], consists of a 10 m tessellated reflector of focal length 7.3 m, making it an $f/0.7$ system. The focal plane detector, or camera, is a hexagonal close-packed array of 109 photomultiplier tubes, which records a 109-pixel image of the Cherenkov light. Over the course of the observations three different configurations of the detector where utilised.

2.1.1. Standard 91+18 camera

For data recorded in 1991 and 1992, the array consisted of an inner hexagonal grid of 91 Hamamatsu R1398 photomultiplier tubes with a 0.25° spacing. Each of these tubes had a photocathode diameter of 2.5 cm and viewed a 0.197° region of the sky. An outer ring of 18 RCA 6342/IV tubes completed the array. These tubes had a 4.27 cm photocathode with an individual field of view of 0.336°. We will refer to this configuration as the *Standard 91+18* camera.

Table 1
Summary of TeV observations

Epoch	Hardware mode	Image analysis technique	Observation mode	Number of scans	Duration (hours)
Oct 1991	*Standard 91 + 18*	*Supercuts* *Extended Supercuts*	ON–OFF	29	13.8
Sep–Oct 1992	*Standard 91 + 18*	*Supercuts* *Extended Supercuts*	Tracking	31	22.9
Oct 1993	*Standard 109*	*Supercuts* *Extended Supercuts*	Tracking	7	4.5
July–Sep 1995	*Standard 109*	*Supercuts 95* *Extended Supercuts* *Small Events*	Tracking	26	11.9
Oct 1995	*Hybrid-UV 109*	*UV Analysis*	Tracking	34	15.6
Total				127	68.7

2.1.2. *Standard 109 camera*

For observations made during the 1993 season and in July to September 1995, the outer ring of larger tubes was replaced with a partial ring of 18 2.5 cm tubes to give the *Standard 109* configuration.

2.1.3. *Hybrid-UV camera*

Finally data were recorded in October 1995 using the *Hybrid-UV* camera. This used a visible blocking filter to allow observations during Moon-lit time. A liquid filter was used to block wavelengths above 350 nm. This was used in conjunction with the Hamamatsu R1398 tubes of the *Standard 109* camera to give sensitivity in the 200–350 nm region [14].

In each of these detector configurations each individual tube was ac-coupled into an amplifier which in turn was fanned out to separate discriminators and analogue-to-digital converters. The system was triggered when 2 out of the inner 91 tubes exceeded a threshold corresponding to about 50 photoelectrons. A digitised 109-pixel image was then recorded. The conversion to digital counts (dc) was approximately 1 dc $\approx$ 1 photoelectron [15].

2.2. *Observation modes*

The observations were carried out in either an ON–OFF mode or a continuous TRACKING mode. In the ON–OFF mode the object was tracked for 28 min, after which the telescope was slewed to a comparison region 30 min later in right ascension. The comparison region was then tracked for 28 min through the same range of azimuth and elevation. These 28 min observation segments are hereafter referred to as scans. Alternatively, a comparison OFF-source region can be tracked prior to tracking the ON-source region. We can use the ON-source/OFF-source scan pairs thus produced to test for an excess of candidate gamma-ray events from the ON-source region. This is an appropriate mode for detecting a steady unpulsed TeV signal, often referred to as a DC signal, such as that from the Crab Nebula [10]. The presence within the field of view of the fourth magnitude star 71-Aql requires that a number of photomultiplier tubes (typically 3) are switched off in hardware, in order to avoid excessive tube currents. Any tubes switched off during the ON-source observation were also switched off during the corresponding OFF-source observation.

In the continuous tracking mode the instrument was used to observe the suspected source continuously, maximising our exposure to the source but at the cost of having no OFF-source data for comparison. This mode is preferred for surveying candidate sources where it is suspected that the TeV signal is either periodic or episodic. The tracking scans vary in length from $\sim$ 28 to $\sim$ 60 min.

2.3. *Data analysis techniques*

The pixel gains were first normalised using images recorded from a nitrogen flash lamp which uniformly illuminated the camera. Any pixel which exceeded

4.25 times the night sky noise fluctuation in that channel were classified belonging to the image picture. Pixels which adjoined picture pixels and exceeded 2.25 times the sky noise fluctuation were classified as forming the image boundary. The remaining pixels were classified as being part of the background and were set to zero. This gains normalisation and noise reduction procedure is described by Fegan [16].

The resulting cleaned and normalised images are approximately elliptical and may then be described by simple moment fitting parameters [17]. The shape of the image is described by the dimensions of the semi-major and semi-minor axes which are referred to as the image *length* and *width*. The orientation of the image may be described by *alpha*, the angle between the major axis and a line connecting the centroid of the image with the centre of the field of view. In addition, the *size* parameter measures the total number of digital counts in the image, the *distance* parameter measures the displacement of the centroid from the centre of the field of view, and the *frac*3 parameter measures the fraction of the total image *size* which falls in the three most intense pixels. Images of gamma-ray induced events tend to be more compact and have smaller values of *length* and *width* than those of background cosmic ray events. The orientation parameter *alpha* may be used to preferentially select events whose origin was at the centre of the field of view, i.e. in the direction of the putative source.

Five different sets of parameter selection criteria have been used. The different sets of criteria are appropriate to different hardware configurations and to different shower energy regions. In general, the different methods involve some pre-selection to reject random noise triggered events followed by the selection of gamma-like events on the basis of their shape and orientation parameters. The criteria are summarized in Tables 2 and 3.

2.3.1. Supercuts analysis

The *Supercuts* technique was developed for the *Standard 91+18* system. Pre-selection consists of a software trigger requiring light intensity in at least two pixels to exceed 40 dc, and also *frac*3 < 0.975. The *frac*3 filter has the effect of eliminating events which result from cosmic ray muons which pass through the camera. The parameter ranges for the shape and orientation cuts were optimized using the signal from the Crab Nebula as observed in the 1988–89 season [18]. The energy threshold of the instrument was ~ 500 GeV for observations close to the zenith. This threshold increases with zenith angle [19]. Typically, the observations of AE-Aqr were carried out at a zenith angle of 35 degrees. This increases the energy threshold by 80% to ~ 900 GeV.

2.3.2. Supercuts 95 analysis

Prior to the 1995 observing season, the high voltage settings were raised to 1.4 times their previous values and discriminator levels were increased by 20%. In addition, the minor facets were re-coated. This reduced the energy threshold of the instrument near the zenith to ~ 200 GeV. The trigger rate increased from approximately 5 events per second to 15 events per second. The reduction in energy threshold introduced two new sources of background into the data. The telescope could now be triggered by fluctuations in the night sky background or by Cherenkov light from single local muons. Therefore, *Supercuts 95* applies a modified image pre-selection. Image *sizes* must exceed 400 dc and the first and second highest pixel intensities recorded in the image must be 100 dc and 80 dc, respectively. The pre-selection raises the effective energy threshold near the zenith to ~ 300 GeV [12].

2.3.3. Small event analysis

A separate analysis technique has been developed to study the smaller events failing the 400 dc cut [20]. For sources with hard spectra, including these small events reduces the overall sensitivity of the instrument. However, for objects which do not emit at higher energies, the *size* > 400 dc cut imposed by *Supercuts 95* may well eliminate the signal. The dominant background amongst the small events is muon triggers. Muon images tend to have low light level per unit arc length and can be discriminated against using a *length*/*size* cut.

2.3.4. Extended supercuts analysis

A disadvantage associated with the *Supercuts* techniques outlined above is that the parameter domains are independent of energy. However, it is known that the *length* and *width* of gamma-ray images increase with primary energy. Essentially, *Supercuts* maximises

Table 2
Summary of event selection techniques

Hardware	Standard 91+18	Standard 109	Standard 109	Hybrid-UV
Selection type	*Supercuts*	*Supercuts-95*	*small events cuts*	*hybrid UV*
pre-selection	$max1 > 40$ dc $max2 > 40$ dc $frac3 < 0.975$	$size > 400$ dc $max1 > 100$ dc $max2 > 80$ dc $frac3 < 0.975$	$size < 400$ dc $max1 > 40$ dc $max2 > 40$ dc $frac3 < 0.975$	$size > 150$ dc $0.30 < frac3 < 0.50$ proximity cut
Distance cut	0.51–1.10°	0.51–1.10°	0.51–1.10°	0.63–1.08°
Shape cut	$0.16° < length < 0.30°$ $0.073° < width < 0.15°$	$0.16° < length < 0.30°$ $0.073° < width < 0.15°$	$length/size < 7.4 \times 10^{-4°}$/dc $0.16° < length < 0.27°$ $0.08° < width < 0.14°$	$hadronicity < 0.10$ $(length - width) < 0.20°$
Orientation cut	$alpha < 0.15°$	$alpha < 0.15°$	$alpha < 0.15°$	$alpha < 20°$
Energy (near zenith)	$<\sim$ 500 GeV	$>\sim$ 300 GeV	$\sim$ 200–$\sim$ 300 GeV	$>\sim$ 1.1 TeV
References	[18]	[12]	[20]	[14]

Table 3
Extended Supercuts criteria for 1995

$|length - 0.991 - 0.054 \log_{10}(size)| < 0.0676$
$|width - 0.136 + 0.060 \log_{10}(size) - .020 \log_{10}(size)^2| < 0.0474$
$\{alpha - 50.714 + 28.189 \log_{10}(size) - 4.26 \log_{10}(size)^2\} < 12.10$

the signal to noise ratio by rejecting higher energy showers. *Extended Supercuts* attempts to increase the sensitivity of the standard camera to higher energy showers. The means for the *length*, *width* and *alpha* parameters can be fitted using second order polynomials in the logarithm of *size*. Images are accepted as candidate gamma-rays if their parameter values fall within a symmetrical range about the *size*-dependent parameter means. The ranges are chosen so that about 95% of simulated gamma-ray images are selected. Due to hardware changes such as mirror degradation, the precise values of the polynomial coefficients and ranges change slightly from one observing season to the next. The values applied to the 1995 data are listed in Table 3. The technique is discussed in detail elsewhere [15].

Extended Supercuts may be important in the context of AE Aqr as the 1 min and 70 min bursts reported by The Durham group [7,8] appear to have contained a larger proportion of higher energy events.

2.3.5. *Hybrid-UV analysis*

Noise rejection and gamma-ray selection techniques have been developed specifically for the hybrid-UV system [14]. By rejecting events which contain less than 150 dc and by demanding that the three most intense pixels in the image occur within 0.75 degrees of one another, spurious events caused by the bright Moon are eliminated. Following the application of this software filter, the event rate is independent of the position of the Moon and is about 2 events per second. Event shape selection is then made on the basis of *hadronicity* and *(length-width)* cuts. *Hadronicity* is a parameter which measures the fraction of the total Cherenkov light which falls within an elliptical template. The orientation cut in the *alpha* parameter is slightly looser than that applied in *Supercuts 95*.

The hybrid-UV camera has been used successfully, during bright moonlight conditions, to detect TeV gamma rays from the Crab Nebula at the 4.9σ level in 10.2 hours of ON-source data and an equal amount of OFF-source data [14]. In addition, the Active Galactic Nucleus Markarian 421 was detected at the 3.9σ level in 7.1 hours ON-source and OFF-source

data [14]. The energy threshold near the zenith is estimated to be 1.1 TeV. The sensitivity of the hybrid camera is about 30% that of the standard camera.

3. Results

We have applied five different analysis types to our data: a search for a steady DC excess, a period search on a scan-by-scan basis, an incoherent periodicity analysis, a coherent periodicity analysis and a search for burst activity on a time scale of 1 min.

3.1. DC analysis

Observations from October 1991 consist of 29 data pairs recorded in the ON–OFF mode. These may be analyzed for the presence of a DC signal. If N_{ON} is the number of gamma-like events from the ON-source data, and N_{OFF} is the number from the comparison OFF-source data, then the statistical significance of any excess events observed from the ON region is

$$n_{sigma} = \frac{N_{ON} - \gamma N_{OFF}}{\sqrt{N_{ON} + \gamma^2 N_{OFF} + \Delta\gamma^2 {N_{OFF}}^2}}. \quad (1)$$

Here, $\gamma \pm \Delta\gamma$, referred to as the tracking ratio, is the time spent observing the ON region divided by that spent observing the OFF region. In this analysis $\gamma = 1$ and $\Delta\gamma = 0$. Table 4 lists the N_{ON} and N_{OFF} values for data selected separately by image shape and orientation, and for the combined *Supercuts* selection. There is no evidence for significant continuous steady emission. Likewise, there is no evidence for any individual hot scans. The distribution of the n_{sigma} values on an pair-by-pair basis is given in Fig. 1 and indicates no evidence for significant emission in any individual scans. An upper limit for a steady TeV flux can be determined using the method of Helene [21]. Assuming a collection area of 6.5×10^8 cm^2 for observations at a zenith angle of 35 degrees, the upper limit at an energy threshold of 900 GeV is 4.0×10^{-12} photons cm^{-2}s^{-1} at 99.9% confidence level. We have also applied an ON–OFF analysis to events selected using *Extended Supercuts* in order to increase our sensitivity at higher energies. The results are listed in Table 4 and again there is no evidence for the presence of a steady signal.

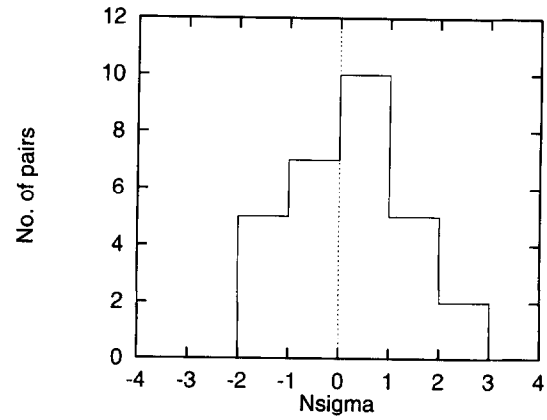

Fig. 1. The distribution of significances of the DC excesses for the 29 ON–OFF data pairs in the 1991 dataset.

As the data recorded in years other than 1991 were in the tracking mode we are unable to apply an ON–OFF type analysis to it. Taking data may be used to search for a DC signal level using the *alpha* type analysis discussed by Catanese et al. [22]. The *alpha* analysis estimates the background by using those events which pass all the *Supercuts* criteria except orientation. Events for which *alpha* $< 15°$ should contain any signal events and form the ON-source data. Events for which $20° <$ *alpha* $< 65°$ are used as the background or OFF-source data. The tracking ratio γ must be determined from contemporaneous non-source data. However, this method does not work in cases such as AE Aqr where there is a bright star within the field of view, which can distort the *alpha* distribution and make the determination of γ from independent data difficult.

3.2. Scan-by-scan periodic analysis

The arrival time of each event was corrected to the Solar System barycentre using the JPL DE200 ephemeris. The precision of the timing hardware and barycentering software has been verified by carrying out optical observations of the Crab Pulsar using the Multiple Mirror Telescope, located near the 10 m gamma-ray telescope at the Whipple Observatory. The optical signal was fed through the 10 m electronics and software, and the light curve reconstructed [23]. Given the relatively long period of AE Aqr, barycentering will only become important in a coherent periodic analysis. We then applied a Rayleigh analysis to the data, on a scan-by-scan basis, over the frequency

Table 4
DC analysis of 1991 dataset

Selection	N_{ON}	N_{OFF}	$N_{ON} - N_{OFF}$	n_{sigma}
Raw	86816	87380	−564	−1.35
Supercuts shape	3047	3091	−44	−0.56
Supercuts orientation	7730	7856	−126	−1.01
Supercuts shape + orient.	586	566	20	+0.59
Extended Supercuts	1539	1543	−5	−0.09

intervals [29.85 mHz, 30.40 mHz] and [59.70 mHz, 60.80 mHz] using 100 trial frequencies in each interval. These ranges contain the first and second harmonics of the white dwarf frequency as well as the QPO's reported by the Potchefstroom group [5,6]. The analysis was applied to gamma-like events selected using each of the appropriate methods for each observing epoch as listed in Table 1. The maximum Rayleigh power obtained amongst all these searches was 6.99, corresponding to a chance probability of 9.2×10^{-4}. The following degrees of freedom must be taken into account: the sum of the products of the number of scans and number of selection techniques over the entire database is 246; the average scan length is 32.5 min so that the period search intervals have a width of 2.12 independent Fourier frequencies; we have searched at 2 harmonics of the White Dwarf period; the oversampling factor is ~ 2. When these are included, the maximum Rayleigh power obtained is consistent with a random background.

We have constructed a Rayleigh power distribution by determining the powers at six independent periods, representative of the search ranges, specifically 29.85 mHz, 30.13 mHz, 30.40 mHz, 59.70 mHz, 60.25 mHz and 60.80 mHz. We have applied this to the data using each of the event selection methods listed in Table 1, giving a total of 1476 power values. Fig. 2 illustrates the integral distribution of power values. There is no significant deviation from the power law distribution of slope −1 associated with randomly distributed events.

3.3. Incoherent periodic analysis

The Rayleigh powers from the 127 individual data scans have been combined incoherently using the method described by Lewis [24]. In an initial analysis, gamma-like events were selected using the *Supercuts, Supercuts-95* and *Hybrid-UV* criteria where appropriate. In a second analysis *Extended Supercuts* was used instead of ordinary *Supercuts*. The smallest probability in the frequency search range was found using the initial analysis. The occurred at a frequency of 59.96 mHz and returned a probability of 7.1×10^{-3}. Taking into account the degrees of freedom (selection types = 2, Fourier frequencies = 2.12, harmonics = 2, oversampling = 2), this is not significant.

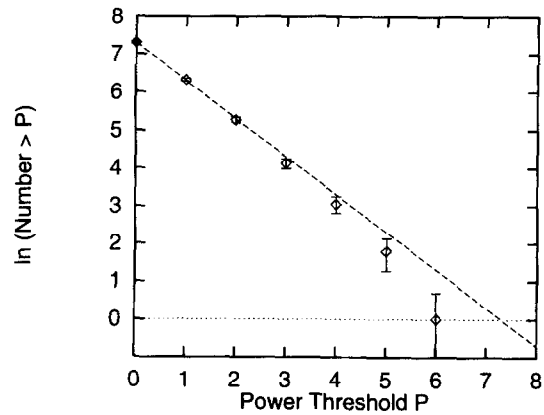

Fig. 2. The integral distribution of Rayleigh power values. The straight line of slope −1 shows the expected distribution for randomly distributed events.

It is of interest to plot the cumulative incoherent probability as a function of scan number as shown in Fig. 3. While at no stage does the probability reach a level which, having considered all degrees of freedom, could be considered in itself to be significant, the behaviour at 59.96 mHz is reminiscent of that observed by the Pochefstroom [5,6] albeit at the first harmonic. They report that the shape of the cumulative probabilities suggests that approximately one out of ten of their observation contains a pulsed signal. The sharp increase in the cumulative probability in our 1995 data

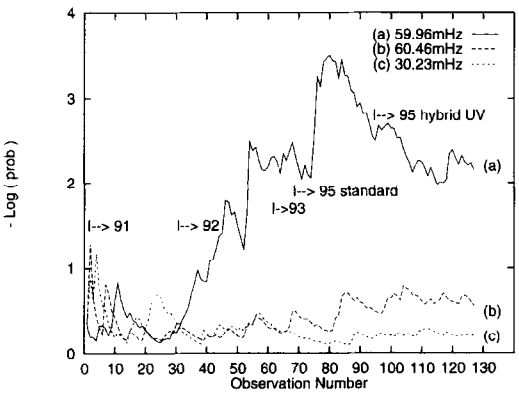

Fig. 3. The cumulative incoherently summed probability as a function of observation number. The probabilities are those calculated using the method of Lewis [24] before the degrees of freedom discussed in the text are considered.

is confined to two out of the twenty nine scans taken that season and we have used an *alpha* analysis of this data to test if these two scans contain an excess of gamma-like events [22]. We can compare the number of events for which $0° < alpha < 15°$ with those for which $20° < alpha < 65°$. The tracking ratio γ has been determined from looking at the distribution of *alpha* values in the remaining twenty seven scans from that year, which do not contribute to the increase in cumulative probability. Since in this case we have determined γ using data recorded on the same object, the presence of a bright star within the field of view does not pose a problem. We obtained the following values: $N_{0-15} = 83$, $N_{20-65} = 274$, and $\gamma = 0.303 \pm 0.017$. Eq. (1) returns a value of $n_{\text{sigma}} = 0.0$. Thus there is no evidence for an increase in number of gamma-like events in these two scans.

3.4. Coherent periodic analysis

We have combined the data sets coherently by epoch folding at the first and second harmonics using the ephemeris of DeJager et al. [3], which incorporates a period derivative term. We have also allowed for the orbital motion using the same ephemeris. Gamma-like events were selected using the *Supercuts*, *Supercuts-95*, and *hybrid-UV*, and also using *Extended Supercuts*. There is no evidence for any coherent pulsed emission at either harmonic. The light curve reported by the Durham group for pulsed emission during the 70 min burst [8] suggests a pulse width of $\sim$ 30%. Within each light curve we have selected the 30% of the period which contains the most events and using the Helene method [21] have calculated upper limits for the *Supercuts* selected data at an energy threshold at 900 GeV. At the 99.9% confidence level these limits are 1.5×10^{-12} photons $\text{cm}^{-2}\text{s}^{-1}$ at both F_0 and at F_1.

3.5. Burst analysis

To search for burst activity on the time scale of minutes, we moved a 60 s window through each scan in steps of 12 s. In each scan, and for each selection technique, we noted the maximum number of events that occurred in a 60 s window. We then used a Monte Carlo algorithm to calculate the probability of such an occurrence happening by chance given the average event rate in that scan, where the average is calculated after excluding the peak 60 s interval. The most improbable such grouping of events had a chance probability for that scan of 3.6×10^{-3}. Given that 246 such searches took place, this is consistent with a random background. Based on an average event rate of 1.2 min^{-1} for the *Supercuts* selected data, we calculate an upper limit for 1 min bursts during our observations of 3×10^{-10} photons $\text{cm}^{-2}\text{s}^{-1}$ at an energy threshold of 900 GeV and at a confidence level of 99.9%.

3.6. Optical data

For the four nights of 17–20th October 1992 we made simultaneous optical and TeV observations. The optical observations were carried out using the nearby Whipple Observatory 1.2 m telescope and reveal one occasion per night in which the object brightness temporarily increased by approximately one half magnitude. The durations of these flares ranged from 5 min up to 25 min. We see no evidence for any TeV activity during these observations, so we are unable to test for any correlation between TeV and optical activity.

4. Conclusion

A detailed analysis of 68.7 hours of data recorded on AE Aqr has revealed no evidence for any steady, pulsed or episodic TeV emission. Owing to the different longitudes of the Whipple, Potchefstroom and Durham observing sites simultaneous observations be-

tween groups are not possible. In October of 1991 and again in October of 1992 our observations overlap with those of the Durham group to the extent that we carried out some observations on the same dates. However, TeV activity was not reported by either group during these months. We do not have any such overlap with the observations of the Potchefstroom group.

Confirming infrequent burst activity will always be difficult. The Durham group detected two significant TeV bursts in $\sim$ 172 hours of observation while the Potchefstroom group saw two bursts in rapid succession in $\sim$ 308 hour of data. If we assume a simple Poisson model for the distribution of such activity there is a 0.7 probability of finding no bursts in our 68.7 hours of observations. Thus our results are not inconsistent with the reports of the other groups who have seen evidence for relatively infrequent TeV activity in larger databases. Our upper limit for the TeV flux from AE-Aqr in the quiescent state is three orders of magnitude less than the flux reported for the 1 min burst detected by the Durham group [7]. Thus the burst activity represents a very significant increase in TeV emission.

Acknowledgements

We acknowledge the technical assistance of K. Harris and the help of the Whipple Observatory support staff. This work has been supported by grants from U.S. Department of Energy, PPARC in U.K. and Forbairt in Ireland.

References

[1] E.L. Robinson, A.W. Shafter, S. Balachandran, Astrophys. J. 374 (1991) 298.
[2] W.F. Welsh, K. Horne, J.B. Oke, Astrophys. J. 406 (1993) 229.
[3] O.C. DeJager et al., Mon. Not. R. Astron. Soc. 267 (1994) 577.
[4] J. Paterson et al., Astrophys. J. 240 (1980) L133.
[5] P.J. Meintjes et al., Astrophys. J. 401 (1992) 325.
[6] P.J. Meintjes et al., Astrophys. J. 434 (1994) 292.
[7] C.C.G. Bowden et al., Astropart. Phys. 1 (1992) 47.
[8] P.M. Chadwick et al., Astropart. Phys. 4 (1995) 99.
[9] M.F. Cawley, T.C. Weekes, Exp. Astron. 6 (1995) 7.
[10] G. Vacanti et al., Astrophys. J. 377 (1991) 467.
[11] M. Punch et al., Nature 358 (1992) 477.
[12] J. Quinn et al., Astrophys. J. 456 (1996) L83.
[13] M.F. Cawley et al., Exp. Astron. 1 (3) (1990) 173.
[14] M. Chantell et al., Astropart. Phys. 6 (1997) 205.
[15] G. Mohanty et al., Astrophys. J. (1997), submitted.
[16] D.J. Fegan, Space Sci. Rev. 75 (1996) 137.
[17] A.M. Hillas, Proc. 19th ICRC, La Jolla, Vol. 3 (1985) 445.
[18] M. Punch et al., Proc 22nd ICRC, Dublin, Vol. 1 (1991) 464.
[19] F. Krennrich et al., Astrophys. J. 481 (1997) 758.
[20] P. Moriarty et al., Astropart. Phys. 7 (1997) 315.
[21] O. Helene, N.I.M. 212 (1983) 319.
[22] M. Catanese et al., Astrophys. J. (1997), submitted.
[23] G.H. Gillanders et al., Proc. 25th ICRC, Durban, Vol. 3 (1997) 185.
[24] D.A. Lewis, Statistical Methods for Physical Science, J.L. Stanford, S.B. Vardeman, eds. (Academic Press, 1993).